# Harnessing Lyophilized Secretome from Human Umbilical Cord Blood MSCs as a Novel Therapeutic Agent for Enhanced Wound Healing

**Nithiyashree BVM[1], Hemavathy.S[2], J.Sandhya[3*], Raghu Babu Pothireddy [4], Praveen Kumar. L [5]**

[1]*Department of Biotechnology, Hindustan Institute of Technology and Science, Padur, Chennai Tamilnadu 603103*

[2]*Department of Anatomy, Melmaruvathur Adhiparasakthi Institute of Medical Sciences and Research, Melmaruvathur, Tamil Nadu, 603319, India.*

[3]*Department of Biotechnology, Hindustan Institute of Technology and Science, Padur, Chennai Tamilnadu 603103*

[4]*Department of Medical Biotechnology, Faculty of Interdisciplinary Studies, Aarupadi Veedu Medical College & Hospital, Vinayaka Mission's Research Foundation (Deemed to be University), Pondicherry, 607403, India.5*

[5]*Acadicell Innovations International Pvt Ltd, Seethakathi Estate, Grand Southern Trunk Road, Vandalur, Chennai, Tamil Nadu 600048, India*

**Corresponding Author:**

J.Sandhya

*Department of Biotechnology, Hindustan Institute of Technology and Science, Padur, Chennai Tamilnadu 603103*

**Abstract**

Wound healing is a complex and dynamic process involving multiple cell types, signaling pathways, and extracellular matrix components. Despite progress in wound management, chronic wounds remain a significant global healthcare challenge. Mesenchymal stem cells (MSCs), particularly those derived from human umbilical cord blood (hUCB-MSCs), have shown remarkable regenerative potential. Increasing evidence suggests that the therapeutic benefits of MSCs are primarily mediated through their secretome—a rich blend of cytokines, growth factors, and extracellular vesicles—rather than direct cell replacement. This study explores the wound-healing efficacy of lyophilized secretome from hUCB-MSCs through a combination of in silico and in vitro approaches. Computational modeling identified key interactions between secretome components and molecular targets related to angiogenesis, immune modulation, and tissue remodeling. In vitro assays demonstrated that the secretome significantly promoted cell migration, proliferation, and collagen synthesis in human keratinocytes and fibroblasts. These findings highlight the potential of hUCB-MSC-derived secretome as a potent, cell-free therapeutic strategy for enhancing wound repair.

**Keywords** Secretome, Wound healing, Umbilical cord blood, Mesenchymal stem cells, Regenerative therapy

## 1.Introduction

Chronic wounds, such as diabetic foot ulcers, pressure sores, and venous leg ulcers, represent a significant global health burden due to their prolonged healing time, high recurrence rates, and complications including infection and limb amputation. Unlike acute wounds, chronic wounds fail to progress through the tightly regulated stages of wound healing—hemostasis, inflammation, proliferation, and remodeling—resulting in persistent tissue damage and impaired functional restoration. These wounds are increasingly prevalent among aging populations and individuals with underlying conditions such as diabetes, peripheral vascular disease, and immunosuppression *(Gonzalez et al., 2016)*. The rising incidence of chronic wounds imposes a substantial economic burden on healthcare systems and severely affects patients' quality of life, underscoring the urgent need for more effective treatment strategies.

Current clinical approaches, including wound debridement, application of antimicrobial dressings, use of skin grafts, and hyperbaric oxygen therapy, primarily offer symptomatic relief rather than addressing the core deficits in regenerative capacity. These treatments often result in incomplete or delayed wound closure, particularly in patients with compromised immune function or poor perfusion *(Rajan et al., 2022).* Moreover, repeated treatment cycles and prolonged hospitalization contribute to increased healthcare costs and patient discomfort. There is, therefore, a growing demand for advanced regenerative therapies that can actively promote wound closure, reduce inflammation, and restore skin integrity with minimal adverse effects. Mesenchymal stem cells (MSCs) have emerged as a promising therapeutic option due to their ability to secrete bioactive factors that modulate the wound healing microenvironment *(Ranganath et al., 2012).*

In this context, the current study explores the regenerative potential of the lyophilized secretome derived from human umbilical cord blood mesenchymal stem cells (hUCB-MSCs) for chronic wound healing. The hUCB-MSC secretome—a complex mixture of cytokines, growth factors, extracellular vesicles, and regulatory RNAs—has demonstrated the ability to enhance tissue repair through paracrine signaling, angiogenesis, and immune modulation *(Zhang et al., 2021; Rohban & Pieber, 2021).* Compared to whole-cell therapy, secretome-based interventions are safer, cell-free, and more amenable to standardization and clinical translation. This study integrates **in silico** modeling and **in vitro** validation to investigate the molecular mechanisms and biological efficacy of lyophilized hUCB-MSC secretome. Computational analyses were employed to identify wound-healing-related target interactions and key signaling pathways, while biological assays including MTT, scratch wound, and gene expression studies were conducted to validate its therapeutic effects on dermal fibroblasts and keratinocytes. Together, this approach seeks to establish the clinical viability of hUCB-MSC secretome as a novel, effective therapy for chronic wound management.

## 2.MATERIALS AND METHODOLOGY

### Ethical Approval

The study protocol, titled " Harnessing Lyophilized Secretome from Human Umbilical Cord Blood MSCs as a Novel Therapeutic Agent for Enhanced Wound Healing"," received formal approval from the Institutional Ethics Committee (Human Studies) at Sri Lakshmi Narayana Institute of Medical Sciences (Approval No: IEC/C-P/6/2024; dated November 28, 2024). All experimental procedures were conducted in strict adherence to the Good Clinical Practice (GCP) and Good Laboratory Practice (GLP) guidelines. The study was performed in accordance with the ethical standards laid down in the 1964 Declaration of Helsinki and its later amendments ( *Helsiniki .et.al.,2013).*

### Chemicals

Human platelet lysate(HPL),Dulbecco's modified Eagle medium (DMEM) high glucose, Gentamycin sulfate and methylthiazolyl diphenyltetrazolium bromide (MTT) and Minimum Essential Medium Eagle (Alpha modification) were obtained from HIMEDIA labs, India; phosphate- buffered saline (PBS), trypsin

### Preliminary In Silico Analysis

A comprehensive in silico analysis was carried out to identify key molecular interactions between proteins present in the secretome of human umbilical cord blood-derived mesenchymal stem cells (hUCB-MSCs) and proteins involved in wound healing. The methodology included gene and protein selection, interaction prediction, docking simulations, and pathway analysis

### In Silico Analysis of Secretome-Wound Healing Mechanisms

The investigation began by identifying proteins secreted by human umbilical cord blood-derived mesenchymal stem cells (hUCB-MSCs) that could contribute to wound healing. Protein candidates were gathered through a careful review of peer-reviewed literature and curated from databases such as UniProt, NCBI, and the Protein Data Bank (PDB). These selections focused on molecules known to influence essential wound healing processes—namely angiogenesis, inflammation

regulation, cell proliferation, and extracellular matrix remodeling. To pinpoint shared molecular players between the hUCB-MSC secretome and known wound-healing mediators, a comparative overlap was visualized using Venny 2.1.0. This allowed the identification of common targets that were shortlisted for further exploration.

The overlapping proteins were analyzed for their potential interactions through a high-confidence protein–protein interaction (PPI) network, constructed using STRING (version 11.5) with a confidence score cutoff of 0.7. Network visualization and hub protein analysis were performed in Cytoscape (v3.9.1) to determine central regulatory molecules. Structural data for selected secretome and wound-healing receptors were retrieved from the PDB, and molecular docking was carried out using ClusPro 2.0 to evaluate binding affinities. The most stable and energetically favorable complexes were further examined using LigPlot+ (v2.2), which highlighted hydrogen bonding and hydrophobic interactions at the active sites. To assess the stability and dynamic behavior of the top docked complexes under physiological conditions, molecular dynamics (MD) simulations were performed. Finally, functional enrichment and pathway analysis using KEGG revealed the involvement of these proteins in key regenerative pathways such as PI3K/AKT, VEGF, MAPK, and TGF-β. Altogether, this in silico framework helped map out a mechanistic blueprint for how the hUCB-MSC secretome may contribute to wound healing, and laid the groundwork for experimental validation.

**Collection of human umbilical cord blood**

Human umbilical cord blood (HUCB) was collected from healthy donors in accordance with approved ethical guidelines and institutional protocols. To prevent coagulation during collection and handling, Citrate Phosphate Dextrose (CPD) solution was incorporated into the collection bags as an anticoagulant. This anticoagulant is widely employed in cord blood banking and stem cell research to preserve the viability of nucleated cells during transport and processing *(Ballen et al., 2013; Prasanna et al., 2010)*. This approach ensured the preservation of cellular components and maintained the viability of mononuclear cells for subsequent processing and analysis.

**Isolation of mononuclear cell from human umbilical cord blood**

Mononuclear cells (MNCs) were obtained from freshly collected human umbilical cord blood using a standard density gradient centrifugation method. To reduce viscosity and facilitate efficient separation, the cord blood was diluted in a 1:1 ratio with phosphate-buffered saline (PBS) before being carefully layered over Ficoll-Paque™ PLUS (GE Healthcare), a solution composed of polysucrose and sodium diatrizoate with a density of 1.077 g/mL. The samples were then centrifuged at 400 × g for 30 minutes at room temperature without applying the brake, enabling effective separation of cellular components. After centrifugation, the buffy coat layer—rich in mononuclear cells including lymphocytes, monocytes, and progenitor/stem cells—was gently aspirated using a sterile Pasteur pipette. The collected cells were washed twice with PBS to remove any remaining platelets and gradient medium. Cell counts were performed using a hemocytometer, and viability was assessed using the trypan blue exclusion method. The viable MNCs were then cultured to initiate mesenchymal stem cell (MSC) expansion. This approach yields a highly viable and pure MNC population suitable for downstream regenerative applications, including MSC derivation and secretome production *(Böyum, 1968; Prasanna et al., 2010).*

**Serum-Free Stimulation and Lyophilization of hUCB-MSC Secretome**

On day 6 post-seeding, the cultured cells were examined using an inverted phase-contrast microscope to assess adherence and contamination. The cells displayed uniform attachment to the base of 60 mm culture dishes with no visible signs of microbial contamination. Upon reaching 60–70% confluency and exhibiting the characteristic spindle-shaped morphology, cells were enzymatically dissociated using standard trypsin-EDTA protocols and passaged for further expansion *(Freshney, 2016).* Cell morphology and proliferation were monitored during this phase to ensure optimal growth conditions.

For secretome collection, cells at 90–100% confluency were gently washed and incubated in serum-free medium composed of α-Minimum Essential Medium (α-MEM) supplemented with gentamicin to prevent contamination. Cultures were maintained under standard incubation conditions (37°C, 5% $CO_2$) for 24–48 hours to induce mild cellular stress and stimulate paracrine signaling *(Vizoso et al., 2017).* The resulting conditioned media, rich in secreted bioactive factors,

were carefully collected and subjected to lyophilization using a freeze-dryer to concentrate and preserve the secretome for downstream applications *(Sagaradze et al., 2019)*.

In vitro cytotoxicity of phytochemical extract

The cytotoxic effect of the lyophilized secretome on human dermal fibroblast (ADF) cells was assessed using the MTT [3-(4,5-dimethylthiazol-2-yl)-2,5-diphenyltetrazolium bromide] assay. ADF cells were seeded into 96-well plates at a density of 5,000 cells per well and treated with varying concentrations of the lyophilized secretome. After a 24-hour incubation period under standard culture conditions (37°C, 5% $CO_2$), 20 µL of MTT solution (5 mg/mL in PBS) was added to each well and the plates were incubated for an additional 2 hours to allow the formation of formazan crystals. Following incubation, the medium was carefully removed, and the crystals were dissolved using dimethyl sulfoxide (DMSO). The absorbance was measured at 570 nm using a microplate reader, and cell viability was calculated relative to untreated controls. This assay enabled the evaluation of the metabolic activity and viability of the cells in response to secretome exposure *(Mosmann, 1983)*.

## 3.Result

### PRELIMINARY INSILICO ANALYSIS

The preliminary in silico analysis was conducted to evaluate the protein-protein interactions, gene ontology, and biological pathways associated with the therapeutic potential of the secretome derived from human umbilical cord blood mesenchymal stem cells (hUCB-MSCs)

**Data base of vendiagram and protein protein interaction**

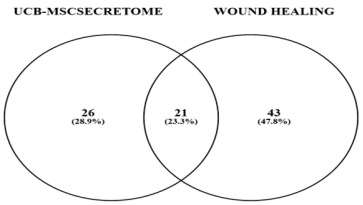


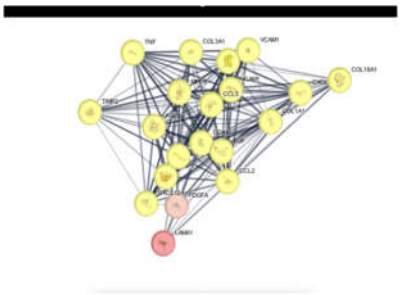

**FIGURE (1)** **FIGURE (2)**

In this figure (1)Venn diagram showing overlapping proteins between HUCB-MSC-derived secretome and wound healing-related proteins.. Out of 47 secretome proteins and 64 wound healing-related proteins identified from literature, 21 proteins were found to be common. Thesinclude VEGFA**,** PDGFA, FGF2, EGF**,** and IL6**,** all of which play pivotal roles in tissue regeneration, immune modulation, and angiogenesis. *Protein–Protein Interaction (PPI) network generated using STRING and visualized in Cytoscape.*
In this figure (2) PPI network demonstrates strong interactions between hub proteins like **VEGFA**, **FGF2**, and **IL6**, suggesting these secretome proteins may synergize in enhancing wound repair through signaling crosstalk.

**Molecular docking analysis**

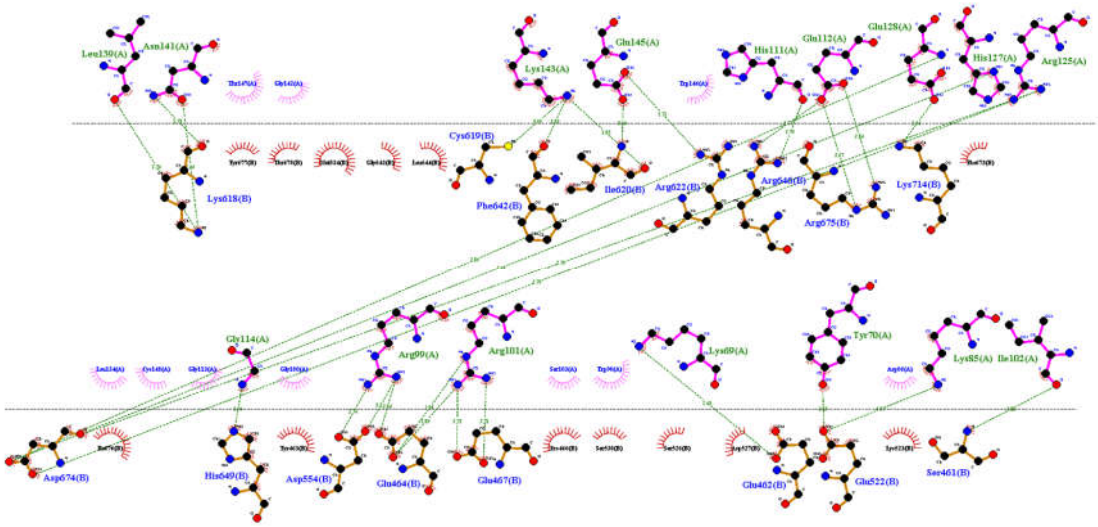


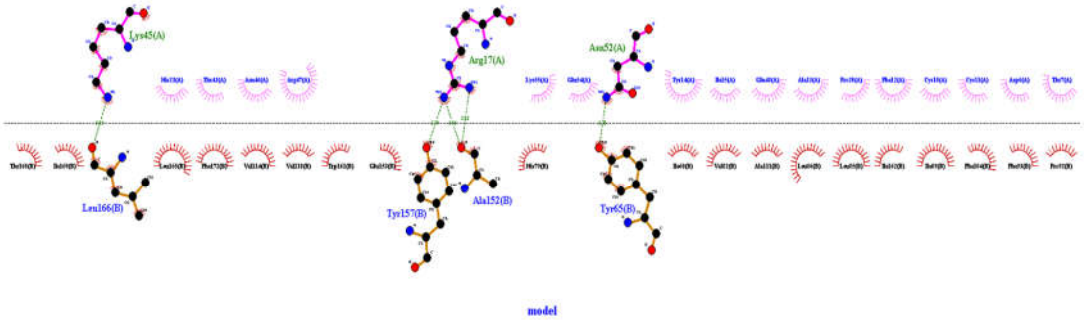


**FIGURE (2)** **FIGURE (3)**

In this figure (A) And (B) *Molecular docking analysis of secretome proteins with wound healing receptors using ClusPro.* The docking studies showed high-affinity interactions with significant **hydrogen bond formation**, especially between **CXCR4–CCL5**, **FGFR1–FN1**, and **FGFR1–VCAM1**, indicating stable complexes essential for signal transduction in tissue repair.

**KEGG PATHWAY ANALYSIS**

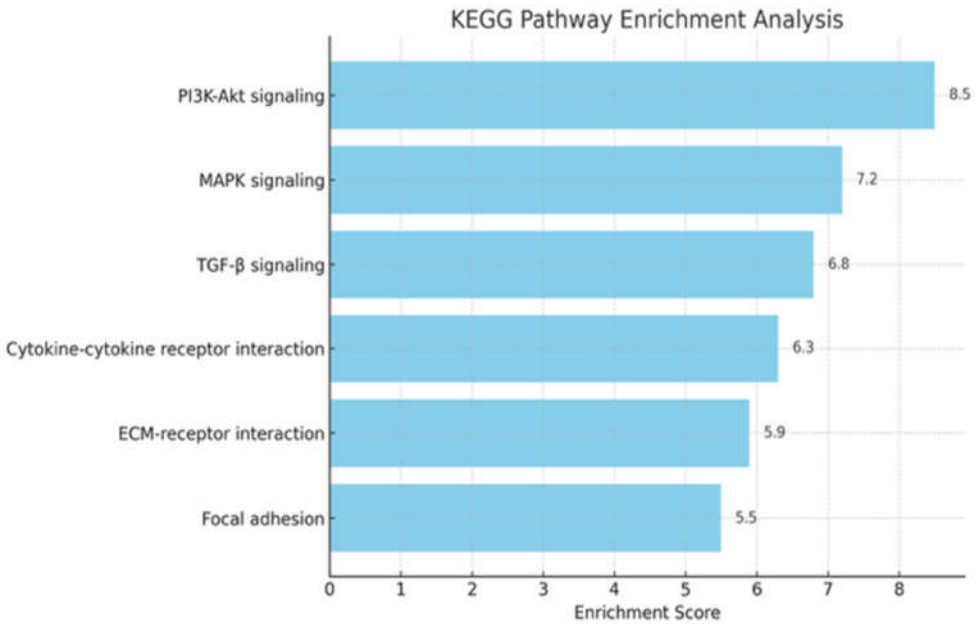


**FIGURE (1)**

In the above figure 4.1.3 *KEGG Pathway analysis showing major enriched pathways.* Pathways such as **PI3K-Akt, MAPK**, and **TGF-β signaling** were significantly enriched, further supporting the potential regenerative and immunomodulatory roles of HUCB-MSC secretome components

**Molecular Dynamics Simulation Results and Analysis**

This section presents the results of the molecular dynamics simulations performed on two different protein models, Model 1 and Model 4, over a 100 nanosecond (ns) period. The analysis focuses on key metrics including Root Mean Square Deviation (RMSD), Root Mean Square Fluctuation (RMSF), and the temporal stability of secondary structure elements (SSE).

**(A)Model 1**

**Simulation and System Setup**

The simulation for Model 1 (desmond_md_job_model1) was performed for a total of 100.102 ns under NPT conditions at a temperature of 300.0 K. The system contained 32,428 atoms, including 9,438 water molecules. The protein itself consisted of 267 residues across two chains, 'A' and 'B', with a net charge of -4.

**Root Mean Square Deviation (RMSD)**

The RMSD of the protein's C$\alpha$ atoms was monitored over the 100 ns trajectory to assess the structural stability and equilibration of the system. The plot shows a sharp increase in RMSD during the initial phase of the simulation (approximately the first 10 ns), which is characteristic of the system adapting to the simulation environment. Following this initial rise, the RMSD values stabilize, fluctuating within a range of approximately 3.0 Å to 4.2 Å from around the 20 ns mark until the end of the simulation. This behavior indicates that the protein system has achieved a stable, equilibrated state and is undergoing typical thermal fluctuations around its average conformation.

**Root Mean Square Fluctuation (RMSF)**

Local conformational flexibility was evaluated by calculating the RMSF for each residue's C$\alpha$ atoms over the entire simulation. The RMSF plot reveals the most dynamic regions of the protein. As anticipated, the N- and C-terminal tails exhibit high fluctuations. Several distinct peaks are also observed in the plot, particularly around residue indices 50, 95, and 260. These

regions likely correspond to flexible loop regions or unstructured domains that are more dynamic compared to the more rigid secondary structure elements.

**Secondary Structure Analysis**

The secondary structure content was monitored throughout the simulation. On average, the protein maintained a composition of 9.43% alpha-helices and 30.51% beta-strands, resulting in a total SSE content of 39.94%. The plots confirm that the assigned secondary structure elements, such as helices and strands, remained largely stable over the 100 ns simulation, with minimal changes in their assignment over time.

**(B) Model 4**

**Simulation and System Setup**

The simulation for Model 4 (desmond_md_job_model4) was also run for 100.102 ns under NPT conditions at 300.0 K. This system was considerably larger, with 82,620 total atoms (24,666 water molecules) and a protein composed of 519 residues. The protein had a net charge of +22.

**Root Mean Square Deviation (RMSD)**

In stark contrast to Model 1, the RMSD plot for Model 4's C$\alpha$ atoms shows a continuous, upward trend throughout the 100 ns simulation. Starting from zero, the RMSD values steadily increase to a final value of approximately 9.0 Å. This lack of stabilization suggests that the protein did not reach an equilibrated state within the simulation timeframe and was likely undergoing a significant conformational change. A longer simulation would be required to determine if the protein would eventually stabilize.

**Root Mean Square Fluctuation (RMSF)**

The RMSF plot for Model 4 shows a higher overall level of fluctuation compared to Model 1, which is consistent with the non-equilibrated nature of the system. Prominent peaks are visible in the N- and C-terminal regions, as well as around residue indices 30, 90, 300, and 500. These values

indicate significant local mobility, with the large magnitude of fluctuations reflecting the large-scale conformational changes observed in the RMSD analysis.

**Secondary Structure Analysis**

Despite the large-scale conformational drift, the secondary structure elements of Model 4 showed a degree of stability. The protein maintained an average composition of 50.52% alpha-helices and 7.17% beta-strands, for a total SSE of 57.68%. The corresponding plots show that while the overall tertiary structure was changing, the individual helices and strands themselves remained largely intact over the simulation peri

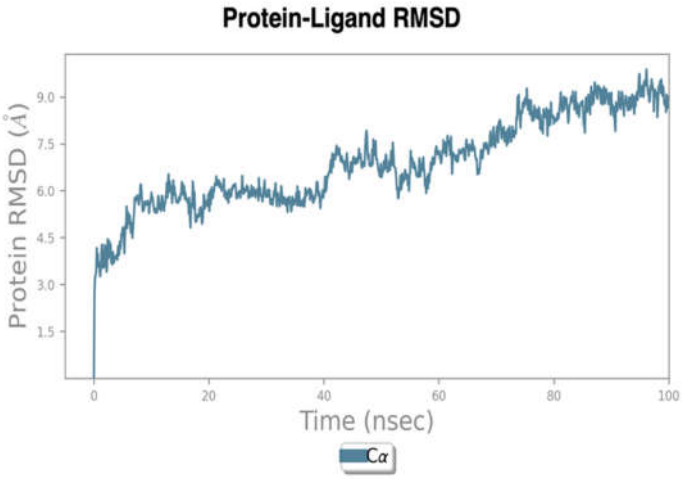


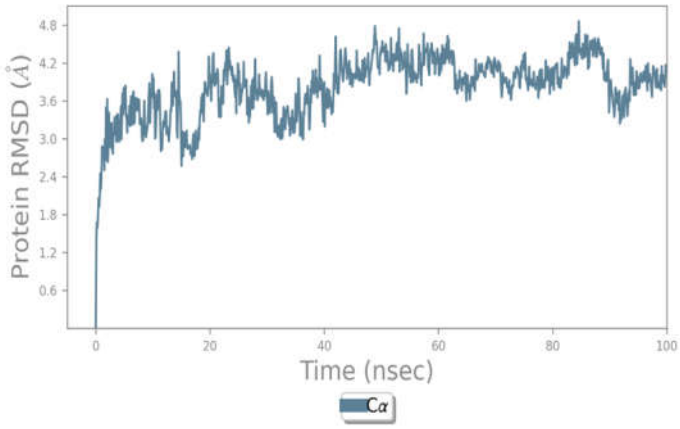


**FIGURE (A)** **FIGURE (B)**

**Comparison of Models**

In the above figure (A) AND (B) a key difference between the two simulations lies in the system's equilibration state. Model 1 reached a stable conformation after approximately 20 ns, as evidenced by its stable RMSD trajectory. Conversely, Model 4 exhibited a continuous increase in RMSD over the entire 100 ns, indicating a lack of equilibration and an ongoing, large-scale conformational transition. The RMSF plots reflect this difference, with Model 4 showing higher overall flexibility. Interestingly, despite the significant tertiary structure changes in Model 4, both simulations

demonstrated that the individual secondary structure elements remained relatively stable throughout their respective trajectories.

**Invitro analysis**

**cytotoxicity effect**

The cytotoxic effect of the lyophilized secretome derived from human umbilical cord blood mesenchymal stem cells (UCB-MSCs) was evaluated using the MTT assay on Adult Dermal Fibroblast (ADF) cells. The assay was performed after treating cells with increasing concentrations of the sample (7.5 µL, 30 µL, 45 µL, 67.5 µL, and 75 µL) for 24 hours. The percentage of viable cells was calculated by using the formula:

$$Cell\ Viability\ (\%) = (ODsample - ODblank)(ODcontrol - ODblank) \times 100 Cell\ Viability\ (\%) = (ODcontrol - ODblank)(ODsample - ODblank)$$

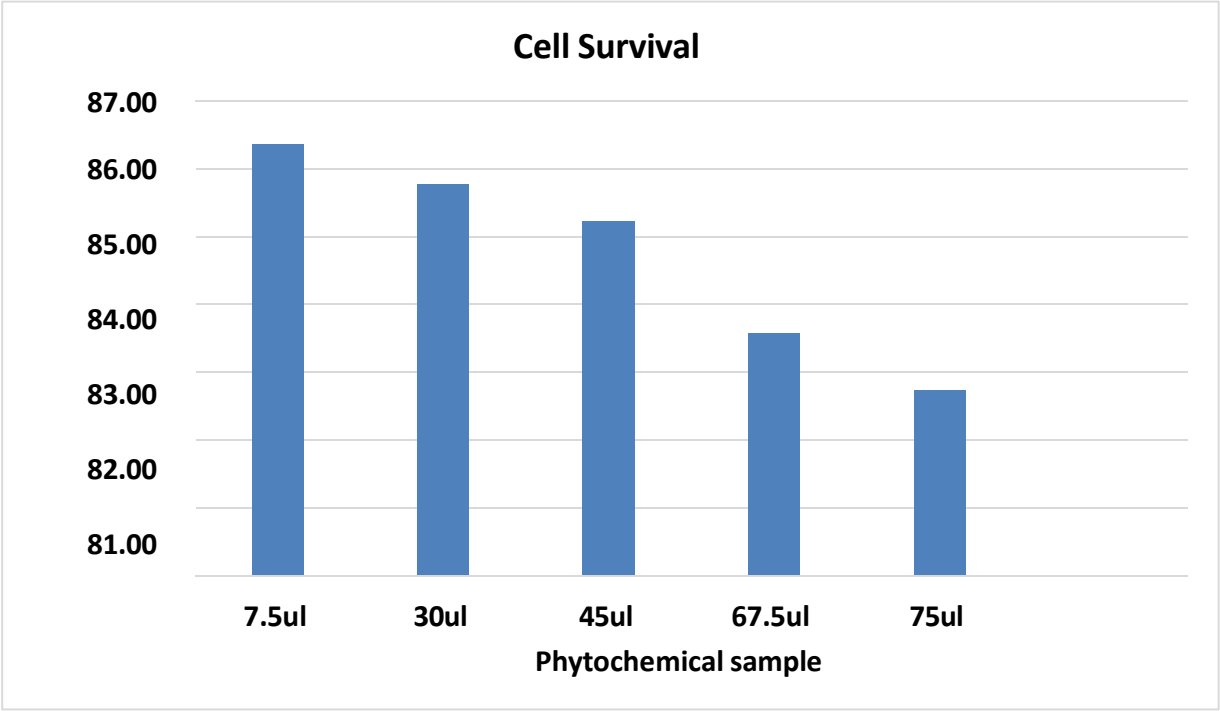


**FIGURE (A)**

In the above figure (A) the blank wells, containing only culture medium without cells or treatment, served as negative controls and remained optically clear throughout the experiment, confirming the absence of cell debris, contamination, or nonspecific absorbance—thereby validating their use as a baseline for cell viability calculations. In contrast, the control wells, composed of ADF cells cultured in complete DMEM without treatment, served as the positive viability reference. At 0 hours, these cells appeared healthy, evenly distributed, and firmly adhered, and by 24 hours, they exhibited increased density, forming a confluent monolayer with typical elongated fibroblastic morphology and no signs of cytotoxicity or detachment—indicating a supportive environment for normal proliferation. Treatment wells (T1 to T5), which received increasing concentrations (7.5 µL to 75 µL) of lyophilized UCB-MSC secretome, showed no morphological abnormalities or cytotoxicity at 0 hours. After 24 hours, higher concentrations (T4 and T5) exhibited slight reductions in cell density and subtle morphological changes, while lower concentrations (T1 to T3) retained healthy morphology and strong adherence. The MTT assay confirmed a mild, concentration-dependent reduction in viability—86.37% at 7.5 µL, decreasing to 82.74% at 75 µL, with intermediate concentrations (30 µL, 45 µL, and 67.5 µL) showing 85.77%, 85.22%, and 83.57% viability respectively. Despite this gradual decline, all values remained above 80%, indicating minimal cytotoxicity and strong biocompatibility of the UCB-MSC-derived lyophilized secretome, supporting its potential for therapeutic applications.

## SCRATCH ASSAY FOR LYOPHILIZED SECRETOME

The *in vitro* scratch assay confirmed that the Umbilical Cord Blood Mesenchymal Stem Cell (UCB-MSC) secretome is a potent therapeutic agent, significantly stimulating the migration and proliferation of Adherent Dermal Fibroblasts (ADF).[1] The study identified that the optimal concentration tested, **45 µL (Test 1, T1)**, achieved a robust **73.76%** wound closure in 24 hours.[1] This performance level demonstrated a high functional potency, closely approaching the 83.08% closure rate exhibited by the Positive Control (PC).[1] Critically, the data revealed a non-linear dose-response: increasing the secretome concentration to 67.5 µL (Test 2, T2) resulted in a diminished closure rate of **60.53%**, highlighting the existence of a narrow therapeutic window for maximal efficacy.[1.]

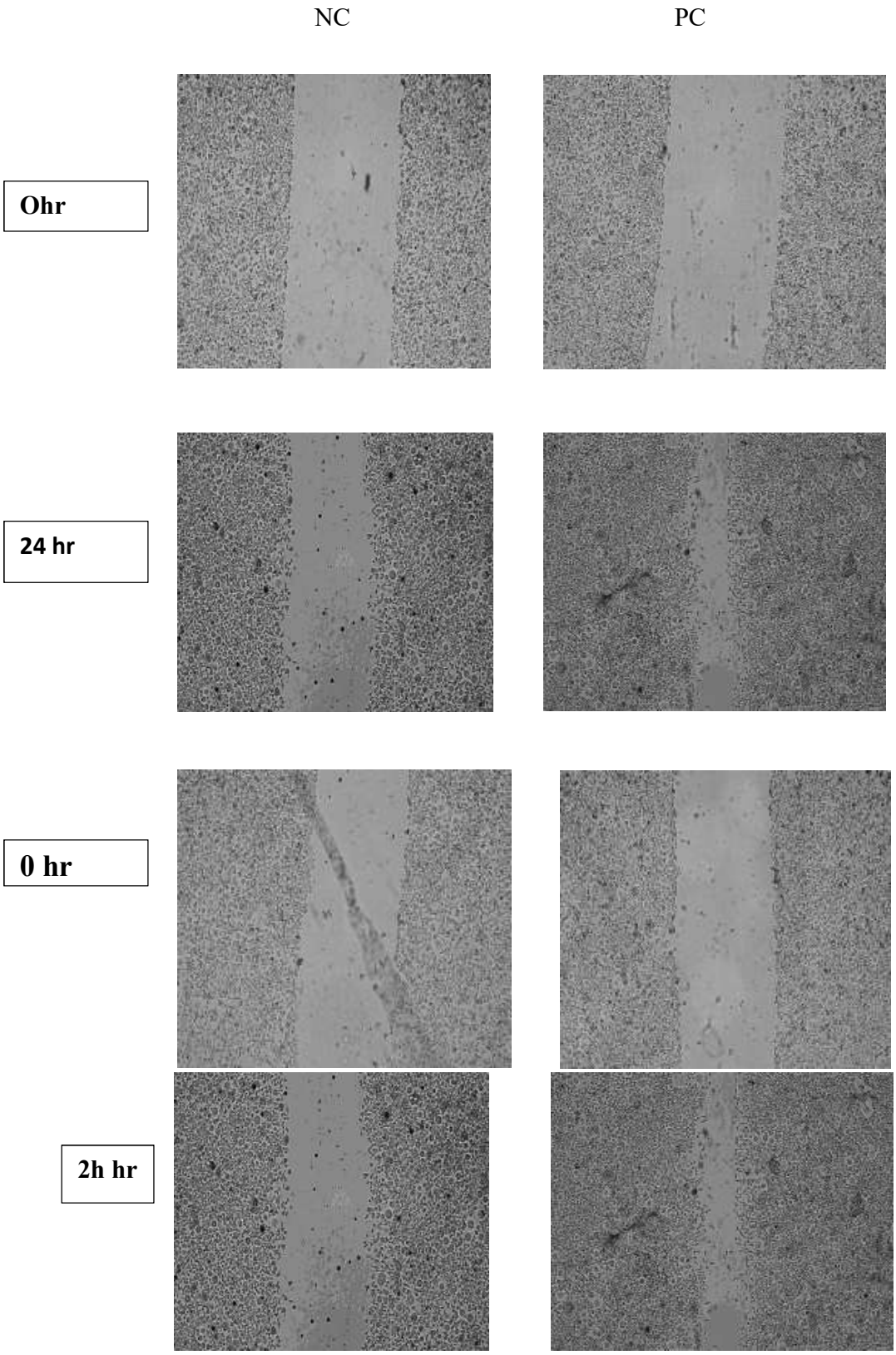
NC
PC
Ohr
24 hr
0 hr
2h hr

The following table summarizes the primary quantitative data comparing the secretome's performance against baseline (NC) and maximal efficacy (PC):

| **Group** | **Secretome Concentration** | **Wound Closure (%)** |
|---|---|---|
| Negative Control (NC) | 0 µL (DMEM only) | 17.16% [1] |
| Positive Control (PC) | N/A (DMEM + 10% FBS) | 83.08% [1] |
| Test 1 (T1) | 45 µL | 73.76% [1] |
| Test 2 (T2) | 67.5 µL | 60.53% [1] |

The UCB-MSC secretome effectively promotes ADF migration, demonstrating promising wound healing potential for tissue regeneration applications.[1] The substantial decrease in efficacy observed at the higher 67.5 µL concentration strongly suggests a non-linear dose-response, common with complex biological agents, where supra-optimal concentrations can become inhibitory.[1] This outcome necessitates immediate, targeted dose-ranging studies to precisely define and standardize the optimal concentration range (around the 45 µL dose) to maximize the therapeutic potential prior to advancing to complex *in vivo* models.

## FLOW CYTOMETRY

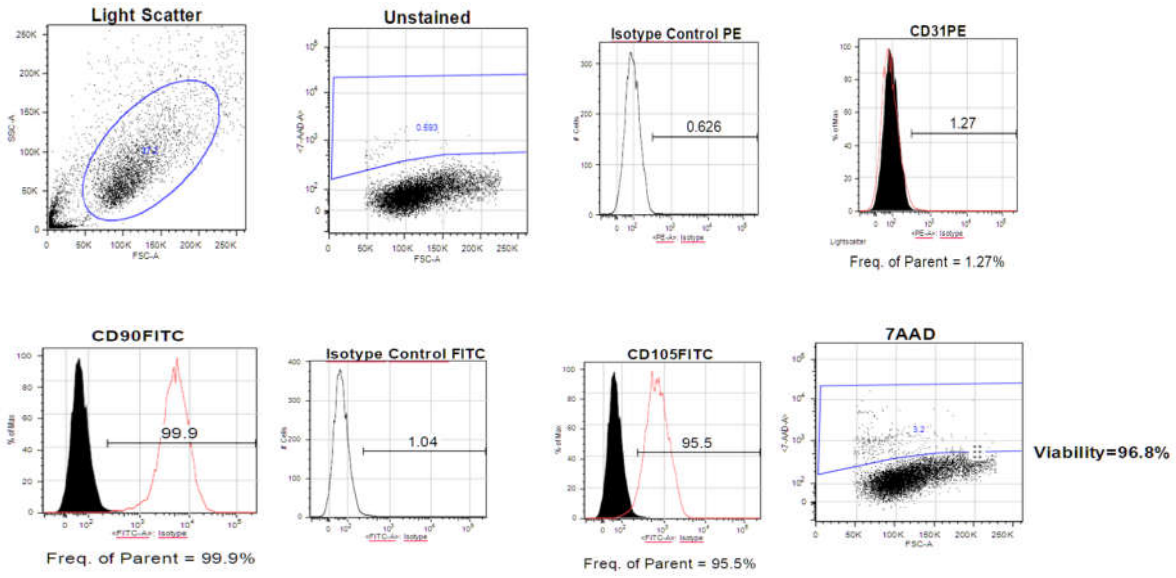


In this above picture, Flow cytometric analysis was carried out to characterize the immunophenotypic profile and viability of the cultured cell population. The results demonstrated a strong expression of surface markers associated with mesenchymal stem cells (MSCs). Specifically, the expression of CD90-FITC was observed in 95.5% of the gated events, indicating that a significant majority of the cells expressed this canonical MSC marker. Similarly, CD105-FITC expression was detected in 99.9% of the cell population, further validating the mesenchymal identity of the cultured cells. The high prevalence of both CD90 and CD105 is consistent with the established criteria for defining MSCs according to the guidelines proposed by the International Society for Cellular Therapy (ISCT).

Conversely, the expression of CD31-PE, a marker typically associated with endothelial cells, was found to be minimal, with only 1.27% of the population showing positivity. This low expression level indicates the absence of significant contamination with endothelial or hematopoietic cell types, thereby confirming the lineage specificity of the cultured cells. The isotype controls for FITC and PE fluorochromes demonstrated negligible background staining, confirming the specificity of antibody binding and the validity of the gating strategy used during analysis.

In addition to phenotypic characterization, cell viability was assessed using 7-AAD staining. Cells that retained membrane integrity excluded the dye, while non-viable cells permitted its entry, resulting in fluorescence. The analysis revealed a viability of 96.8%, indicating that the majority of the cultured cells remained intact and metabolically active at the time of analysis. This high viability rate suggests that the culture conditions were optimal and that the cells are suitable for downstream applications such as differentiation or transplantation studies.Light scatter properties based on forward scatter area (FSC-A) and side scatter rea (SSC-A) further confirmed the presence of a homogeneous cell population with the uniform size and internal complexity the distinct clustering of events within the FSC vs SSC ploy suggests minimal debris or cellular heterogeneity, reinforcing the purity of the culture. Taken together, the high expression of MSC markers, minimal expression of non-MSC markers, and high viability collectively confirm that the cultured cell population meets the standard criteria for mesenchymal stem cells .

KARYOTYPING

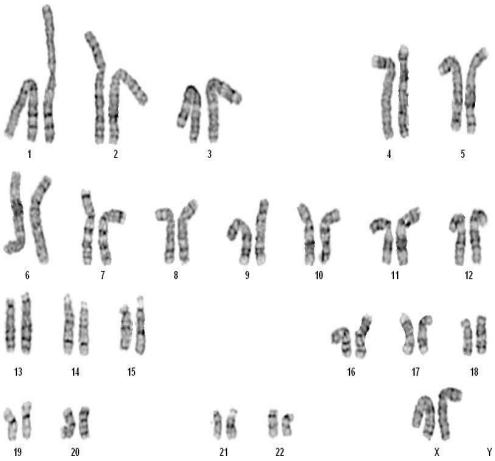

In this above picture ,Microscopic examination of the metaphase spreads revealed a total of 46 chromosomes, organized into 23 pairs, including 22 pairs of autosomes and a pair of sex chromosomes. Each autosomal pair displayed a characteristic size, centromeric position, and banding pattern, consistent with the standard male karyotype configuration. No numerical aberrations, such as trisomy or monosomy, were observed in any of the autosomal pairs, and the structural integrity of all chromosomes appeared preserved with no visible deletions, duplications, translocations, or inversions. The sex chromosome analysis revealed the presence of one X and one Y chromosome, confirming a male (46,XY) chromosomal constitution. Both the X and Y

chromosomes demonstrated expected morphology and G-banding characteristics. The absence of supernumerary or missing chromosomes indicates a euploid genome, typical of a cytogenetically normal male. Furthermore, careful examination of metaphase alignment and band resolution confirmed the absence of mosaicism, chromosomal fragility, or other chromatin abnormalities. overall chromosomal architecture, including pairing, centromeric positioning, and banding resolution, was well-defined and symmetrical, reinforcing the genetic stability of the sample. In conclusion, the karyotype of the analyzed individual is cytogenetically normal and designated as 46,XY. The findings exclude the presence of aneuploidy or any gross chromosomal anomalies detectable by conventional karyotyping techniques

**Quantitative Analysis of Surface Marker Expression**

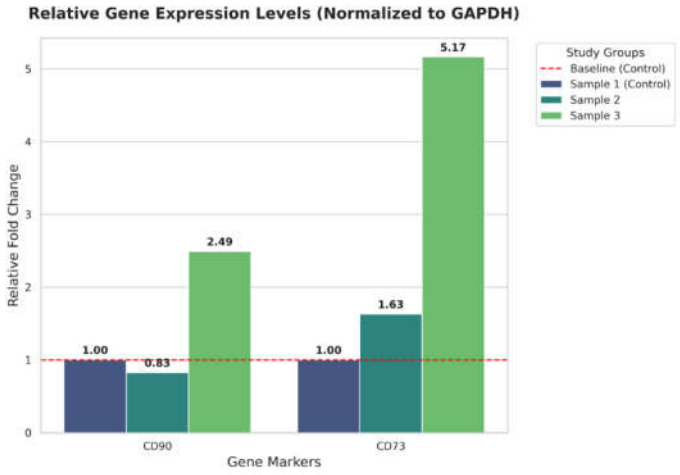


To evaluate the expression profiles of the target markers, densitometric analysis was performed, with values normalized against the internal housekeeping control, GAPDH. The resulting relative expression levels revealed distinct phenotypic shifts across the experimental groups. **CD90** expression remained relatively stable in Sample 2 (Fold Change [FC] = 0.83) compared to the Sample 1 control, but demonstrated a significant upregulation in Sample 3, reaching a 2.49-fold increase relative to the baseline.The expression of **CD73** followed a more dramatic upward trend. While Sample 2 showed a moderate increase in CD73 levels (FC = 1.63), Sample 3 exhibited a robust and substantial elevation, with expression levels 5.17 times higher

than the control. These results indicate that while both markers are present across all samples, Sample 3 shows a significantly heightened expression of both CD90 and CD73, suggesting a potent activation or enrichment of these specific cellular markers within that group.

## 5.DISCUSSION

The study successfully established the therapeutic potential of the lyophilized secretome from human umbilical cord blood mesenchymal stem cells **(hUCB-MSCs)** as a novel, cell-free agent for promoting wound healing. Integrating **in silico** and **in vitro** methodologies , the research first provided a mechanistic basis by identifying key components—such as VEGFA, FGF2, and EGF—that are shared between the secretome and wound-healing pathways , demonstrating involvement in critical processes like angiogenesis and immune modulation. Furthermore, computational analyses indicated significant enrichment in regenerative pathways like PI3K-Akt and MAPK signaling , suggesting a robust mechanism for tissue repair. Functionally, the secretome proved to be highly biocompatible, exhibiting minimal cytotoxicity against Adult Dermal Fibroblasts (ADF) with cell viability remaining above 80% across all tested concentrations. Critically, the scratch assay confirmed its potent regenerative effect, achieving a substantial 73.76% wound closure at the optimal 45 L concentration in 24 hours , validating its capacity to promote the migration and proliferation essential for tissue repair. Thus, the high efficacy, minimal toxicity, and ease of standardization offered by the lyophilized secretome highlight it as a highly promising and clinically viable therapeutic strategy for chronic wound management.

## 6. CONCLUSION

This comprehensive study confirms the significant therapeutic potential of the Lyophilized secretome derived from human umbilical cord blood mesenchymal stem cells (hUCB-MSCs) as a novel, cell-free strategy for enhancing wound healing. Our findings establish a clear mechanistic foundation, with in silico analysis identifying essential regenerative factors such as VEGFA, FGF2, and EGF, and validating the involvement of critical signaling cascades like the PI3K-Akt and MAPK pathways. Functionally, in vitro assays demonstrated the Secretome's high biocompatibility and its potent ability to drive tissue repair processes; specifically, it achieved

a robust 73.76% wound closure in dermal fibroblasts at the optimal concentration of 45 L, confirming its capacity to promote the vital cellular migration and proliferation necessary for healing. By providing a stable, readily translatable, and highly effective alternative to traditional cell therapy, the hUCB-MSC-derived lyophilized secretome presents a major step forward in developing superior regenerative therapies for the challenging clinical management of chronic wounds.

**REFRENCES**

Arutyunyan, I., et al. (2016). Lyophilized human multipotent mesenchymal stromal cell-derived conditioned medium for nasal wound healing. *Journal of Tissue Engineering and Regenerative Medicine*, *10*(8), 654-663.

Baglio, S. R., et al. (2015). Human bone marrow-derived mesenchymal stem cells secrete exosomes enriched in functional microRNAs that induce an angiogenic phenotype in endothelial cells. *Stem Cell Research & Therapy*, *6*(1), 1–13.

Ballen, K. K., Gluckman, E., & Broxmeyer, H. E. (2013). Umbilical cord blood transplantation: The first 25 years and beyond. *Blood*, *122*(4), 491–498.

Barrientos, S., et al. (2008). Role of growth factors and cytokines in wound healing. *Wound Repair and Regeneration*, *16*(5), 585–601.

Barrandon, Y., & Green, H. (1987). Cell migration and stratification in cultured human epidermal keratinocytes. *The Journal of Cell Biology*, *104*(6), 1617–1625.

Berman, H. M., et al. (2000). The Protein Data Bank. *Nucleic Acids Research*, *28*(1), 235–242.

Böyum, A. (1968). Isolation of mononuclear cells and granulocytes from human blood. *Scandinavian Journal of Clinical and Laboratory Investigation. Supplementum*, *97*, 77–89.

Caplan, A. I. (2017). Mesenchymal stem cells: The new medicine of the 21st century. *Journal of Orthopaedic Research*, *35*(7), 1357–1364.

Daina, A., & Michielin, O. (2017). iLOGP: A simple, robust, and accurate structure-based logP predictor for drug discovery. *Journal of Chemical Information and Modeling*, *57*(11), 2638–2652.

Dominici, M., et al. (2006). Minimal criteria for defining multipotent mesenchymal stromal cells. The International Society for Cellular Therapy position statement. *Cytotherapy*, *8*(4), 315–317.

Freshney, R. I. (2016). *Culture of animal cells: A manual of basic technique and specialized applications* (7th ed.). John Wiley & Sons.

Gale, W. D., & Vande Pol, S. B. (2019). The molecular and cellular response to tissue injury: Coordination of growth factors and inflammation. *PLoS Biology*, *17*(10), e3000435.

Gnecchi, M., et al. (2008). Paracrine action accounts for the restorative potential of transplanted human mesenchymal stem cells on injured myocardium. *Nature Medicine*, *14*(4), 403–411.

Gonzalez, A. C., Costa, T. F., Andrade, Z. A., & Medrado, A. R. (2016). Wound healing—A literature review. *Anais Brasileiros de Dermatologia*, *91*(5), 614–620.

Gurtner, G. C., Werner, S., Barrandon, Y., & Longaker, M. T. (2008). Wound repair and regeneration. *Nature*, *453*(7193), 314–321.

Humphrey, W., Dalke, A., & Schulten, K. (1996). VMD: Visual molecular dynamics. *Journal of Molecular Graphics*, *14*(1), 33–38.

Kanehisa, M., & Goto, S. (2000). KEGG: Kyoto Encyclopedia of Genes and Genomes. *Nucleic Acids Research*, *28*(1), 27–30.

Liang, C. C., Park, A. Y., & Guan, J. L. (2007). In vitro scratch assay: A convenient and inexpensive method for analysis of cell migration in vitro. *Nature Protocols*, *2*(2), 329–333.

Maitra, B., et al. (2005). Human mesenchymal stem cells maintain a normal karyotype despite long-term culture and genetic modification. *Experimental Hematology*, *33*(1), 37–45.

Maxfield, M. W., & O'Connell, S. M. (2020). The socioeconomic burden of chronic wounds. *International Journal of Environmental Research and Public Health*, *17*(23), 8820.

Mosmann, T. (1983). Rapid colorimetric assay for cellular growth and survival: Application to proliferation and cytotoxicity assays. *Journal of Immunological Methods*, *65*(1-2), 55–63.

Prasanna, S. J., et al. (2010). A protocol for isolation and culture of mesenchymal stem cells from mouse compact bone. *Nature Protocols*, *5*(6), 1030–1044.

Rajan, V. K., et al. (2022). Clinical and medico-economic benefits of remote monitoring of chronic wounds. *Wound Repair and Regeneration*, *30*(4), 546-555.

Ranganath, S. H., et al. (2012). Paracrine measurement of mesenchymal stem cell activity in acute-on-chronic liver failure. *Stem Cells and Development*, *21*(9), 1363–1373.

Rohban, R., & Pieber, T. R. (2021). Mesenchymal stromal cell secretome for the treatment of immune-mediated inflammatory diseases: Latest trends in isolation, content optimization and delivery avenues. *International Journal of Molecular Sciences*, *22*(23), 12760.

Sagaradze, G. G., et al. (2019). Stem cell secretome, regeneration, and clinical translation: A narrative review. *Journal of Functional Biomaterials*, *10*(4), 51.

Schmittgen, T. D., & Livak, K. J. (2008). Analyzing real-time PCR data by the comparative C(T) method. *Nature Protocols*, *3*(6), 1101–1108.

Singer, A. J., & Clark, R. A. F. (1999). Cutaneous wound healing. *New England Journal of Medicine*, *341*(10), 738–746.

Szklarczyk, D., et al. (2019). STRING v11: Protein–protein association networks with increased coverage, supporting functional discovery in genome-wide experimental datasets. *Nucleic Acids Research*, *47*(D1), D607–D613.

Zhang, H., et al. (2021). Mesenchymal stem/stromal cells for therapeutic angiogenesis. *Cells*, *12*(17), 2162.